Loan 1022: Constraining glacial ice and water movement using microseismic earthquakes

Alex Brisbourne and Tom Hudson, British Antarctic Survey

Abstract

An array of 13 geophones and CMG-6TD sensors was deployed for two months on Vatnajökull Ice Cap, Iceland, to monitor subglacial seismicity and deeper volcanic seismicity. The main array was deployed on the upstream end of Skeiðarárjökull Glacier to record icequakes from the base of the glacier to investigate the hydrological system using temporal and spatial variation of source mechanisms. For comparison, and to help constrain deeper volcanic seismicity, a smaller sub-array was deployed around the Grimsvötn caldera and a single station was deployed over Bárðarbunga where deeper volcanic activity was known to be present. This seismic array was embedded within a broader array of 3-component seismometers operated by Cambridge University. Data were successfully recorded for up to 52 days although tilt of the 6TD instruments compromises much of their data. Although data are dominated by surface crevassing noise, a number of basal icequakes have been identified which are being used in a cross-correlation event search to identify clusters of events. Once a full event catalogue has been produced, source mechanisms and seismic anisotropy in the ice column will be analysed to constrain ice rheology and dynamics.

1) Introduction

The presence and distribution of meltwater at the base of ice streams in both Antarctica and Greenland significantly influences rates of ice flow and consequently the mass balance. Acceleration and deceleration of Byrd Glacier in Antarctica from 2005-7 has been linked to the discharge of subglacial lakes [*Stearns et al.*, 2008]. *Le Brocq et al.* [2013] identified channels beneath the Filchner-Ronne Ice Shelf, indicating the existence of a channelized hydrological system beneath Antarctic ice streams. Drainage of surface meltwater to the bed of ice streams has been shown to reduce the effective pressure at the ice-base interface and result in accelerated ice-flow [*Iken and Bindschadler*, 1986; *Zwally et al.*, 2002]. Subglacial hydrological systems remain poorly constrained but are generally accepted to develop from hydraulically inefficient structures towards more efficient channel structures which facilitate more rapid flow [e.g., *Kamb*, 1987]. In Greenland, a positive correlation between enhanced summer melting and ice displacement is matched by a subsequent negative correlation with winter displacement, modulating annual dynamic ice loss [*Sole et al.*, 2013]. This unexpected result is explained by the evolution of a large-scale subglacial channel system, which subsequently drains areas of high basal pressure resulting in reduced winter motion.

The aim of this study is to evaluate the potential of microseismic monitoring to characterise subglacial drainage. We acquired data on the accessible Skeiðarárjökull Glacier in Iceland, where a well-developed channelized hydrological system likely exists, to assess the potential for identifying and understanding such systems. Our closely-spaced seismic array (Fig. 1) formed part of a broader array of 3-component seismometers operated by Cambridge University allowing a further possibility of comparing analogous "plumbing systems" and the feasibility of the method for system discrimination, and also monitoring geothermal activity and melt movement in five sub-glacial volcanoes.

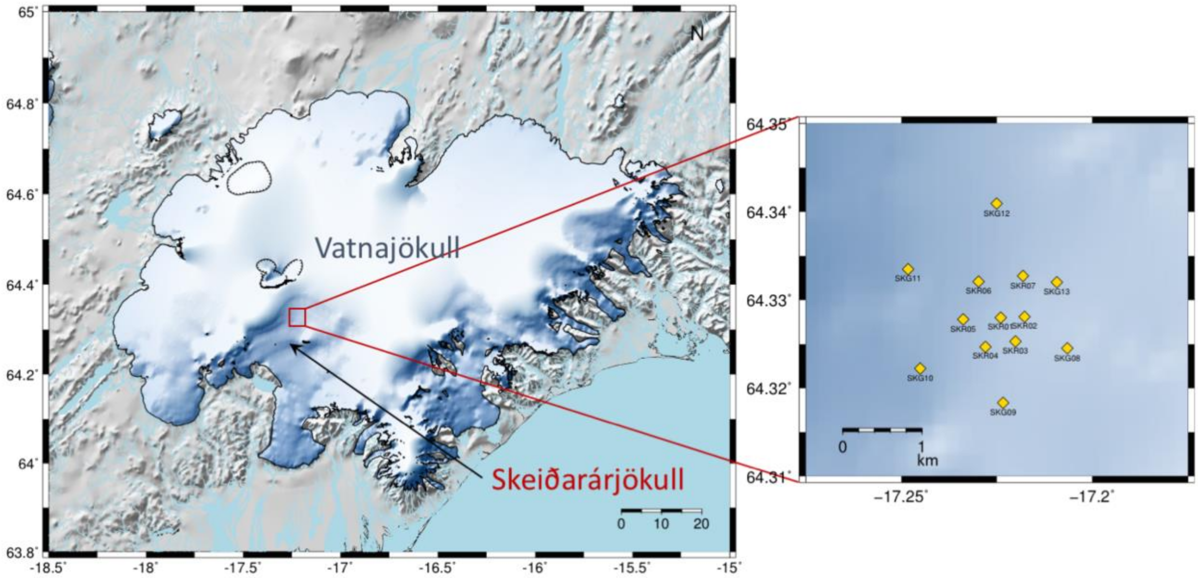

Figure 1. Experiment location and icequake array configuration.

2) Survey procedure

Seven Reftek dataloggers with geophones (four SEIS-UK; three BAS) and six 6TD sensors were deployed in an expanding-spiral shape (Fig. 1) centred on an upstream section of Skeiðarárjökull where ice is thick (increased P-S separation) and fast-flowing (more likely to trigger basal events). Four further 6TD stations were deployed around the Grimsvötn Caldera and one more over Bárðarbunga to provide a comparison of the recording of volcanic seismicity on ice (Appendix 2).

Our deployment methodology was determined by the fact that the experiment was carried out either side of the equilibrium line altitude (ELA) in an area of very high accumulation and melt (up to 5 m). Below the ELA all instrumentation was buried with the sensor at 2-3 m depth and the peripherals closer to the surface. At greater elevation, in the accumulation zone, a sensor burial-depth of 1 m was used. Geophones were placed directly in the snow with 6TDs on a levelled concrete slab (Figs. 2 and 3). The holes were backfilled with snow after deployment. A single 20 W solar panel was deployed at the surface, vertically orientated and facing south. Solar panels were mounted on a 5 m plastic yellow pole rammed into the snow as deep as possible. The panel was attached with an exhaust clamp such that as the snow melted the panel would slide down the pole. As a test, two sites were covered with ablation fleece in an attempt to reduce melting although this did not survive the strong winds. With hindsight, a wooden bar at the base of the solar panel would have been useful to reduce melt-sinking of the solar panel.

SEIS-UK instruments were supplemented by BAS owned Reftek systems and Leica GS10 GPS systems which recorded ice surface motion for the duration of the deployment. Systems were run with continuous GPS at a sample rate of 500 sps (for both the Reftek and 6TD instruments). Site elevations were measured with the BAS-supplied Leica GPS. Vatnajökull is logistically an extremely challenging area to work and requires good local knowledge and collaboration to ensure safe and successful fieldwork.

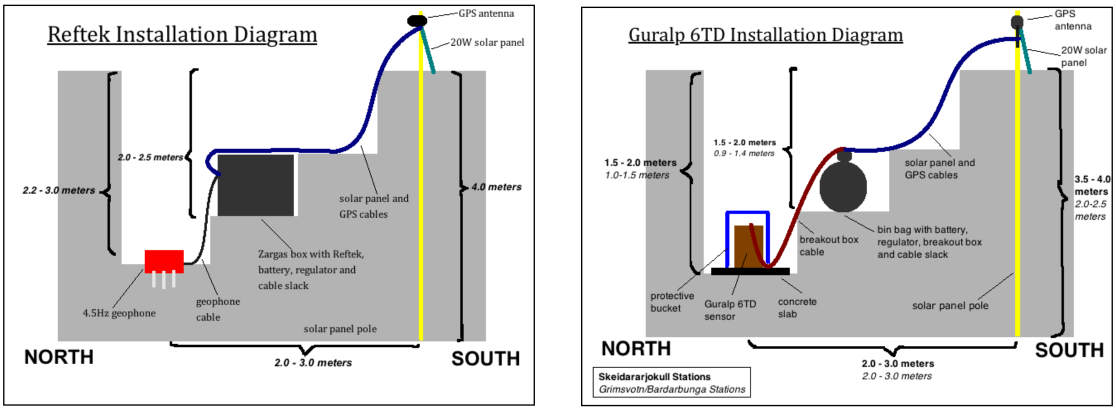

Figure 2. Instrument deployment schematics.

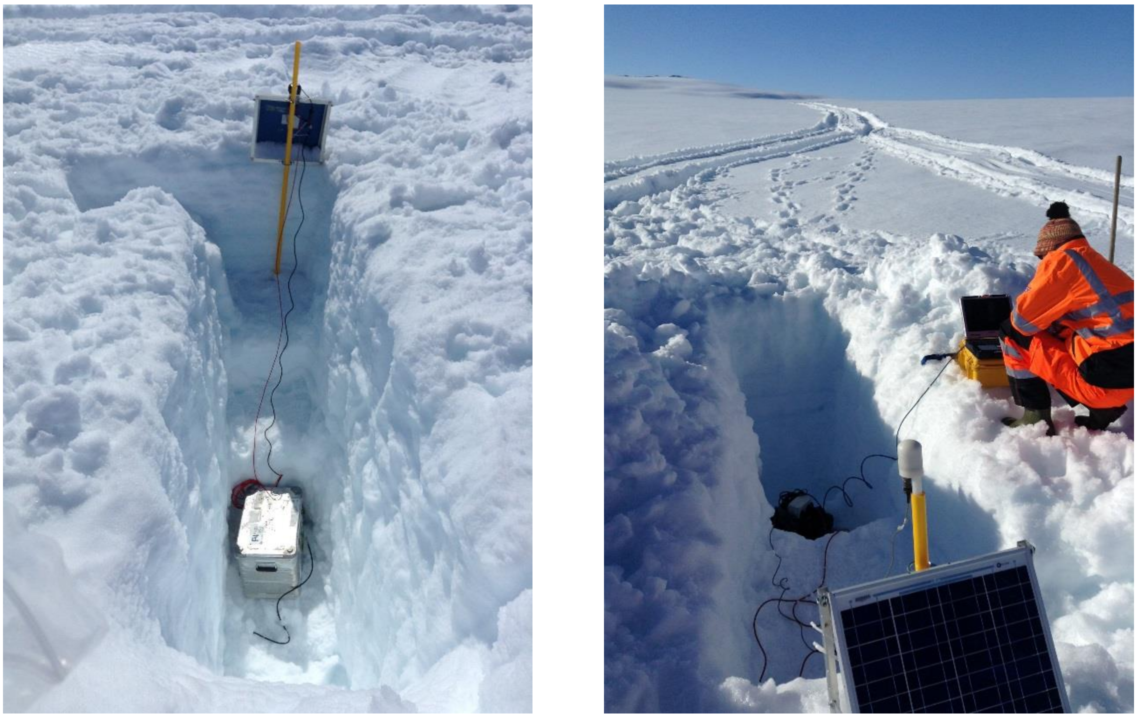

Figure 3. Example Reftek (Left) and 6TD (Right, with Grimsvötn Caldera behind) deployments in 2-3 m holes.

3) Data quality

Background noise is dominated by surface crevassing events with many small events being observed on single stations only and larger events across the entire array (Fig. 4). This makes basal event identification very challenging. Prior to tilt of the sensors the data quality is of sufficient quality that different event types can be identified and event locations determined.

Tilt of the sensors was a major issue below the ablation line. The 6TD sensors proved unable to cope with the conditions and tilted sufficiently to force at least one horizontal component to its end-stops after 3 to 25 days (e.g., Fig. 5). Above the ablation line, snow accumulation was the major issue and sites were buried at retrieval.

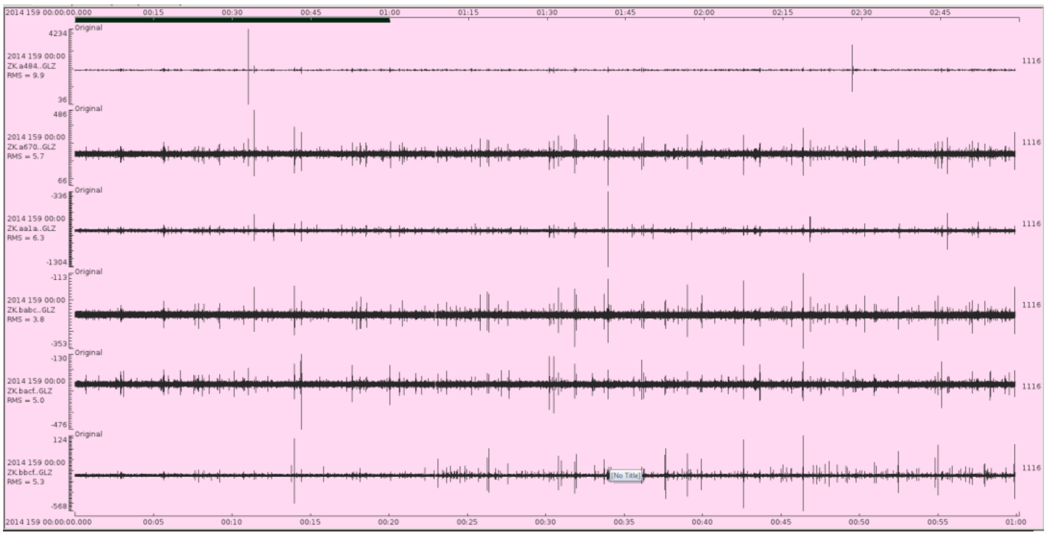

Figure 4. Example one-hour record on the vertical component of six Reftek systems.

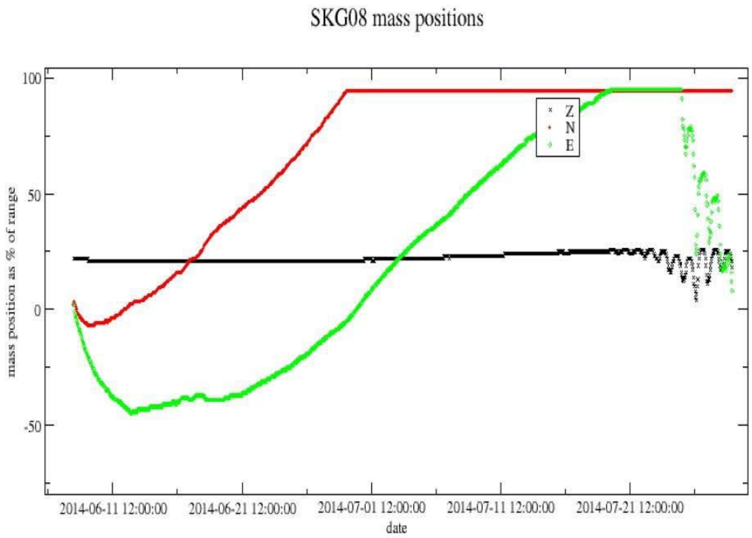

Figure 5. Example of 6TD mass position for the duration of the deployment.

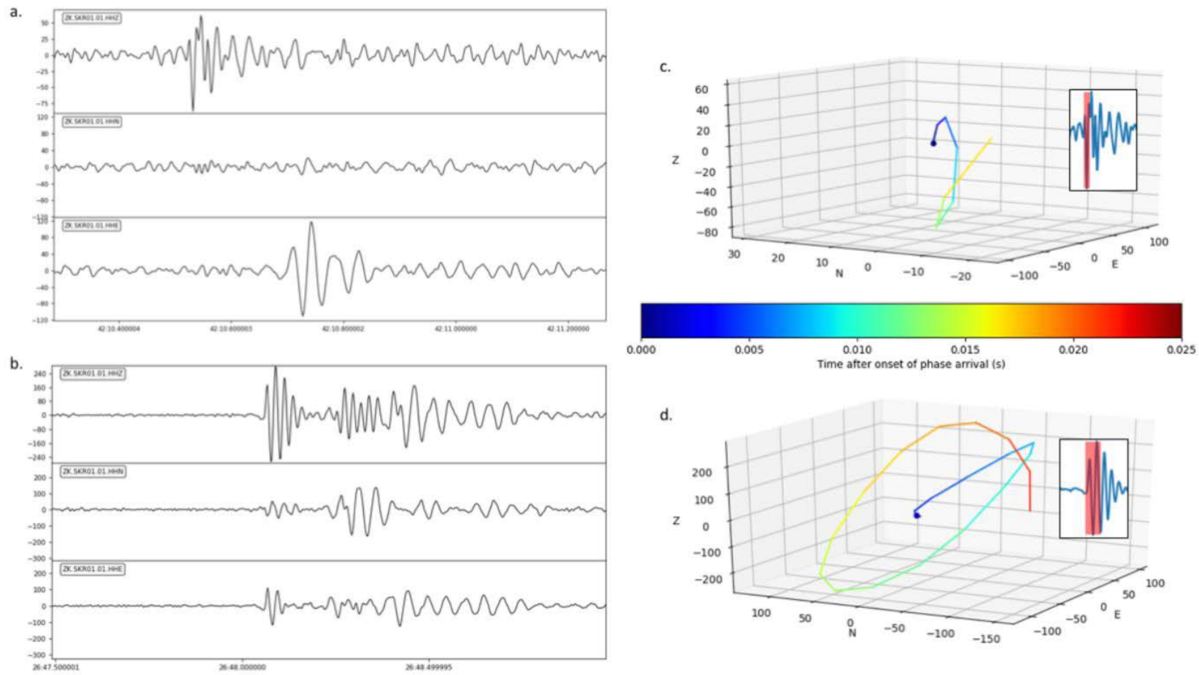

Figure 6. Example basal icequake and surface crevassing event (filtered between 20 to 120 Hz). a. Z, N and E waveforms corresponding to a basal icequake. b. Z, N and E waveforms corresponding to a surface crevassing event. c and d show the particle motions corresponding to the first arrival of each event, for the basal icequake and crevassing event, respectively. The colour of the particle motion plots represents time after the onset of the phase arrival with the blue dot highlighting the first energy.

4) Processing and modelling

These data form a large component of the PhD project of Tom Hudson (Cambridge University DTP joint with BAS: Start date - October 2015; Project title - *Volcano-ice interaction: using microseismicity to probe subglacial processes in Iceland*). Following publication of analogous work on deep volcanic seismicity beneath Bárðarbunga [*Hudson et al.*, 2017], attention has recently switched to the icequake data.

Note: Due to the multi-year time frame involved, the bulk of the data used in the Hudson et al. [2017] study of Bárðarbunga came from other GEF loans, e.g., #968. This loan provided only a fraction of the data used and is therefore not reported in detail here.

The main difficulty with analysing data from settings such as this is identifying basal events from the plethora of surface crevassing noise. We are developing strategies to identify basal events utilising search catalogues determined using tuned STA/LTA trigger algorithms and spectrum based search methods. Any surface crevassing events detected are then automatically removed by looking at the dispersion of the arrival, or the particle motions of the first arrivals observed to check for characteristic surface wave arrivals, such as those in Fig. 5d. Potential basal events are then manually picked and run through non-linear relocation algorithms such as NonLinLoc [Lomax et al, 2000].

5) Preliminary findings and interpretation to date

To-date, 10 basal events have been identified within a 10 day window. Interestingly, using the same procedure on the subsequent 10 day window, no basal events have so far been identified. This result is consistent with observations on Rutford Ice Stream where "sticky spots" of low-porosity sediment are known to cause clusters of seismicity which are temporally intermittent [*Smith et al.*, 2017]. Once a preliminary catalogue of master events has been identified, a cross-correlation search will be carried out to isolate clusters of events.

6) Conclusions and recommendations

- Recording of passive seismicity in glacial settings requires instrumentation which is suitable for the conditions. Sensors which are tilt-sensitive are not worth the effort of deployment without continuous maintenance.
- The masking of basal seismicity by surface crevassing events is a major hindrance to their identification and standard catalogue production methods are not sufficient.
    - Reliable phase identification is the key to event identification.
    - Crevassing events are dominated by high-amplitude Rayleigh wave energy and are generally dispersive.
    - Rather than attempting to tune a triggering routine to automatically isolate basal events (which extremely difficult prior to finding the initial events to ascertain waveforms), we advocate using the distinctive waveforms of surface events to remove these from comprehensive catalogues and then investigating the remainder with particle motion analysis.
- Around 10 basal icequakes have so far been identified in a 10 day period of data. These will be used as master events with a cross-correlation technique to identify clusters of basal seismicity.

7) Further work (PhD outline)

- Produce a basal icequake catalogue for the duration of the deployment.
- Investigate moment tensor solutions and fracture mechanisms.
- Investigate anisotropy of the ice column.

8) Location of the archived data

All data are archived at IRIS DMC (Network code: *ZK 2014*).

9) Publications (including conference presentations)

- Polenet Glacial Seismology Course (poster) – icequake data introduction for discussion.
- Hudson, T. S., R. S. White, T. Greenfield, T. Ágústsdóttir, A. Brisbourne, and R. G. Green (2017), Deep crustal melt plumbing of Bárðarbunga volcano, Iceland, Geophys. Res. Let., 44(17), 8785-8794.

References

Hudson, T. S., R. S. White, T. Greenfield, T. Ágústsdóttir, A. Brisbourne, and R. G. Green (2017), Deep crustal melt plumbing of Bárðarbunga volcano, Iceland, *Geophys. Res. Let.*, *44*(17), 8785-8794.

Iken, A., and R. A. Bindschadler (1986), Combined measurements of subglacial water pressure and surface velocity of Findelengletscher, Switzerland: conclusions about drainage system and sliding mechanism, *J. Glaciol.*, *32*(110), 101-119.

Kamb, B. (1987), Glacier Surge Mechanism Based on Linked Cavity Configuration of the Basal Water Conduit System, *Journal of Geophysical Research-Solid Earth and Planets*, *92*(B9), 9083-9100.

Le Brocq, A. M., et al. (2013), Evidence from ice shelves for channelized meltwater flow beneath the Antarctic Ice Sheet, *Nature Geosci*, *6*(11), 945-948.

Smith, E. C., A. F. Baird, J. M. Kendall, C. Martín, R. S. White, A. M. Brisbourne, and A. M. Smith (2017), Ice fabric in an Antarctic ice stream interpreted from seismic anisotropy, *Geophys. Res. Let.*, *44*(8), 3710-3718.

Sole, A., P. Nienow, I. Bartholomew, D. Mair, T. Cowton, A. Tedstone, and M. A. King (2013), Winter motion mediates dynamic response of the Greenland Ice Sheet to warmer summers, *Geophys. Res. Let.*, *40*(15), 3940-3944.

Stearns, L. A., B. E. Smith, and G. S. Hamilton (2008), Increased flow speed on a large East Antarctic outlet glacier caused by subglacial floods, *Nature Geosci*, *1*(12), 827-831.

Zwally, H. J., W. Abdalati, T. Herring, K. Larson, J. Saba, and K. Steffen (2002), Surface melt-induced acceleration of Greenland ice-sheet flow, *Science*, *297*(5579), 218-222.

Appendix 1

Station Name	Station Type	Latitude (N)	Longitude (W)	Altitude (m)	Deployment Date	Reftek No.	Sensor No.	Digitizer No.
SKR01	Reftek	64.32799	17.22406	1295	07/06/2014	A670	SeisUK3893	N/A
SKR02	Reftek	64.32809	17.21779	1244	07/06/2014	AA1A	SeisUK3447	N/A
SKR03	Reftek	64.32529	17.22019	1231	07/06/2014	A484	SeisUK	N/A
SKR04	Reftek	64.32468	17.22803	1222	07/06/2014	BAS BACF	BAS 1	N/A
SKR05	Reftek	64.3278	17.23388	1221	07/06/2014	BAS BBCF	3106	N/A
SKR06	Reftek	64.33208	17.22983	1299	07/06/2014	BAS BABC	SeisUK3448	N/A
SKR07	Reftek	64.33272	17.21822	1249	08/06/2014	A644	BAS	N/A
SKG08	6TD	64.32452	17.20658	1244	08/06/2014	N/A	T6186	C2077
SKG09	6TD	64.31833	17.22341	1204	08/06/2014	N/A	T6108	946
SKG10	6TD	64.32223	17.24511	1202	08/06/2014	N/A	T6070	C2075
SKG11	6TD	64.33348	17.24828	1239	08/06/2014	N/A	T6051	2426
SKG12	6TD	64.34092	17.2251	1259	08/06/2014	N/A	T6021	2235
SKG13	6TD	64.332	17.20933	1248	08/06/2014	N/A	T6188	949
GR01	6TD	64.38404	17.30489	1632	09/06/2014	N/A	T6112	C2239
GR02	6TD	64.40609	17.42512	1635	09/06/2014	N/A	T6118	C2031
GR03	6TD	64.44107	17.38336	1576	09/06/2014	N/A	T6038	C589
GR04	6TD	64.44749	17.29562	1634	09/06/2014	N/A	T6159	C939
BARD	6TD	64.63947	17.52198	1970	10/06/2014	N/A	T6090	C2081

Table 1. Instrument deployment details

Station	Dates Recording	Julian Days	Days Recording	GB of Data	Notes
	07/06/14 - 30/07/14	158 - 211	54		
SKR01			36	17.8	Refteks (SKR01-07) still being processed;
SKR02			31	15.6	Reftek "Days Recording" estimated
SKR03			53	26.3	from typical 500sps data recording
SKR04			45	22.7	rate of 0.5GB/day
SKR05			52	26.2	
SKR06			52	26.2	
SKR07			52	25.9	
SKG08	08/06/14 - 29/07/14	159 - 210	52	13.1	Full Deployment
SKG09	08/06/14 - 27/06/14	159 - 178	20	4.9	Nothing after 27/06
SKG10	08/06/14 - 29/07/14	159 - 210	52	13	Full Deployment
SKG11	08/06/14 - 29/07/14	159 - 210	52	13	Full Deployment
SKG12	08/06/14 - 29/07/14	159 - 210	52	13	Full Deployment
SKG13	08/06/14 - 29/07/14	159 - 210	52	13	Full Deployment
GR01	09/06/14 - 02/07/14	160 - 183	24	5.9	Nothing after 02/07
GR02	09/06/14 - 02/07/14	160 - 183	24	5.9	Nothing after 02/07
GR03	09/06/14 - 06/07/14	160 - 187	28	7.1	Nothing after 02/07
GR04	09/06/14 - 04/07/14	160 - 185	26	16.9	No reset flash. Ran out of memory after 04/07.
BARD	10/06/14 - 30/06/14	161 - 181	21	5.1	Nothing after 30/06
Refteks: SKR01-07					
Guralp 6TDs*: SKG08-13, GR01-04, BARD					
*Due to the high tilt sensitivity of 6TD horizontal masses, the 6TD horizontal components are not valid for the entire recording period.					

Table 2. Data recording and recovery.

Appendix 2

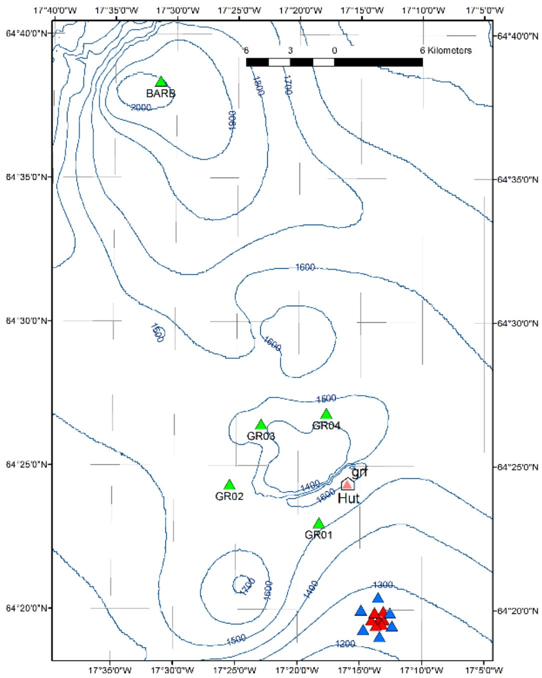

Figure A2. Map of array including stations on Grimsvötn and Bárðarbunga. Red triangles = Reftek; blue = 6TD on icequake array; green = volcanic subsidiary array. GRF is a SIL permanent seismic station.